

## Corrosion Behavior of Copper at Elevated Temperature

Ye Wan<sup>1,2,3,\*</sup>, Xiumei Wang<sup>2</sup>, Hong Sun<sup>1</sup>, Yanbo Li<sup>2</sup>, Ke Zhang<sup>1</sup>, Yuhou Wu<sup>1</sup>

<sup>1</sup> School of Traffic and Mechanical Engineering, Shenyang Jianzhu University, Shenyang 110168, China

<sup>2</sup> School of Materials Science and Engineering, Shenyang Jianzhu University, Shenyang 110168, China

<sup>3</sup> Department of Materials Science and Engineering, University of Virginia, Charlottesville, VA 22904, USA

\*E-mail: [ywan@sjzu.edu.cn](mailto:ywan@sjzu.edu.cn)

Received: 6 July 2012 / Accepted: 3 August 2012 / Published: 1 September 2012

---

Copper is shown to be susceptible to corrosion in the fields of electrical connector contact and thermal nuclear energy. This work aims at assessing the corrosion behavior of copper at elevated temperature via thermoanalytical technique, X-ray diffraction, scanning electron microscopy and coulometric reduction. Cyclic voltammetric was used to identify the corrosion compound of copper and reduction potential. The corrosion mechanism is the formation of the copper oxides. The results shows Cu<sub>2</sub>O and CuO were the corrosion compounds. The initial corrosion of copper is the formation of Cu<sub>2</sub>O, which was converted to CuO in oxygen environment as time going on. For longer exposure time at elevated temperature, two corrosion layers developed on the surface of copper. The inner layer is Cu<sub>2</sub>O and the outer layer is made of Cu<sub>2</sub>O and CuO. Corrosion amount of copper shows an exponential kinetics with temperature.

---

**Keywords:** Copper; Corrosion; Elevated Temperature; Coulometric Reduction

### 1. INTRODUCTION

Copper has been studied extensively in response to its applications and requirement in electrical connector contact and thermal nuclear energy fields due to its high thermal conductivity, excellent electrical conductivity and good workability. However, corrosion of copper must be addressed because copper is susceptible to oxidization in these elevated temperature environments. Corrosion of copper at elevated temperature is a serious problem in aircraft, space structure and power generation equipment and other energy conversion systems. For example, early failures of heat exchanger copper tubes have been recognized not only during service but storage [1]. Boden found Cu-base alloys were susceptible to severe corrosion under boiling heat transfer conditions [2]. The corrosion rate, determined by corrosion mechanism, of copper affects directly the service life at

elevated temperature. Corrosion layers of corrosion products even can flake off due to corrosion and surface film growth and degrade copper. Degradation of copper will make the equipment fail temporarily and is very troublesome. Therefore, the corrosion behavior and the stability of copper in elevated temperature are important and it is necessary to avoid any formation of corrosion products and degradation process of copper in order to prolong its service life via studying the corrosion behavior and the stability of copper.

It is known that there are two corrosion compounds for copper in the oxygen environments:  $\text{Cu}_2\text{O}$  (cuprous oxide) and  $\text{CuO}$  (cupric oxide) [3]. The amount of cuprous oxide and cupric oxide has an essential effect on development of copper corrosion. The scale of  $\text{Cu}_2\text{O}$  and  $\text{CuO}$  formed on Cu in the oxygen environments and at elevated temperature depends on the thermodynamic stability of the oxides [4-7]. Thus it is of interest to examine the thermodynamic aspect of this reaction following by studies of the kinetics, compound and morphological aspects.

Many assessment methods were developed to investigate corrosion of copper, such as thermoanalytical (TA), mass loss, coulometric reduction and other surface examination methods including X-ray diffraction (XRD). Although TA measurement has been used widely to obtain kinetics data [8-12] and the kinetics model can be established fundamentally on the basis of the microscopic measurement of the reaction geometry and the kinetics of the reaction interface advancement [13, 14], it is impossible to get the corrosion compound and the corrosion amount at the same time. Among all those methods, the coulometric reduction method is very useful for characterizing oxide layers on copper surface and performed by many researchers [15-19] because it can be used not only to identify corrosion compounds but also to record reduction time (reduction charge), indicating the corrosion amount, at the same reduction curve.

The work presented here focuses on corrosion of copper at elevated temperature ranging from room temperature to  $900^\circ\text{C}$ . The evolution of the copper oxides and the corrosion kinetics of copper have been investigated to determine the reaction mechanisms via many measurements. The corrosion kinetics was done by thermogravimetric measurement accompanied with coulometric reduction, which provides corrosion amount information of copper. Scanning electron microscopy (SEM) was used to characterize the surface regions of copper at elevated temperatures. The corrosion compound evolutions on copper have been studied via XRD and coulometric reduction and can be explained on the basis of a corrosion mechanism. A two-layer film was examined on the surface of copper.

## 2. EXPERIMENT

*Sample.*— Copper samples (99.999% purity) with the size of  $10\text{ mm} \times 10\text{ mm} \times 2.5\text{ mm}$  (the size is  $1\text{ mm} \times 1\text{ mm} \times 0.5\text{ mm}$  for thermogravimetric analyzing) were polished with SiC paper (successively 600 and 800 grits), cleaned with acetone and rinsed with DI water, dried and kept in desiccators with silica gel for at least 24 hours. High purity water (Millipore  $> 20\text{ M}\Omega\text{ cm}$ ) was used throughout.

*Thermogravimetric (TG) analysis.*— Thermal behavior of copper was carried out on a differential scanning calorimetry (DSC) and thermogravimetric analyzer (STA449F3A, NETZSCH,

Germany) from room temperature to 900°C. The samples were placed in an open alumina pan and heated up to the desired temperature at a preconceived heating rate of 10 °C/min in a flowing compressed air (flow rate was 20 ml/min). The instrumental resolution is 0.1. To calibrate the TG scan, the data curve of an empty sample pan under the identical analysis conditions was made as a baseline file. Isothermal-corrosion was carried out at a constant heating rate of 10°C /min from room temperature to 900°C. TG analysis of the mixture was performed at least in triplicate to assure repeatability of the obtained results.

*Surface examination.* – Corrosion of copper at elevated temperature was conducted in a furnace in air at the desired temperatures followed by XRD, SEM and coulometric reduction. The corrosion products were identified by XRD. XRD data were recorded via a step-scanning diffractometer with Cu Ka radiation (Rigaku D/max-2400, Japan). The morphologies of the samples after exposure were observed using scanning electron microscopy (S-4800, Hitachi, Japan).

*Electrochemical methods.* – A conventional three electrode cell was used for electrochemical studies. The cell exposes a 1 cm<sup>2</sup> portion of the samples to be work electrodes. The counter electrode is a flat platinum mesh. All the potentials were measured against an Hg/Hg<sub>2</sub>Cl<sub>2</sub>/saturated KCl reference electrode. The electrochemical experiments were conducted with potentiostat (PARSTAT 2273, Princeton Applied Research, USA).

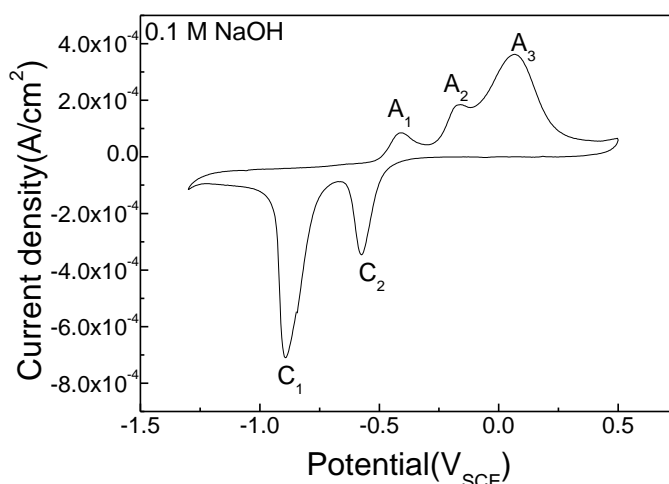
The electrolyte for cyclic voltammetry (CV) was 0.1 M sodium hydroxide, NaOH. According to the recommendation of ASTM B825 [15], potassium chloride (KCl) solution, one of the most common solutions, was used for the coulometric reduction electrolyte where copper oxides were the expected corrosion products. The electrolyte, 0.1 M KCl, for coulometric reduction was prepared in Millipore water and the pH 9 was adjusted by drop-wise addition of 1 M NaOH solution. The pH 9 was selected to decrease the solubility of copper oxide in the reduction electrolyte, which would underestimate the actual amount of copper oxide on the surface of copper. Before the introduction of the electrolyte, the cell itself was flushed with a flow of pure helium for at least ten minutes, and prior to the reduction, the reduction electrolyte was deaerated for at least one hour by bubbling pure helium through the solution to decrease the amount of dissolved oxygen. Current to the sample was applied promptly after addition of the solution to the cell. The current was controlled and the potential was measured with a potentiostat. All the experiments were done by triplicate.

Two values can be ascertained from each reduction curve: the reduction potential and the reduction time, which is from the beginning to the midpoint between the adjacent two potential plateaus. The reduction charge (per unit area, the same below) is calculated from the reduction time multiplied by the reduction current. All the reduction charges were based on the corrosion products being Cu<sub>2</sub>O in the work.

### 3. RESULTS

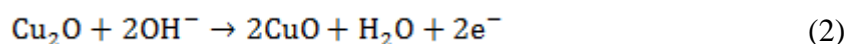
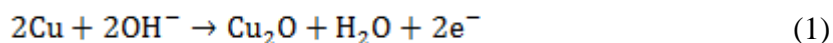
*Identification of corrosion products.* – One of the methods identifying corrosion compounds of copper in this work is reduction potential. Corrosion of copper and the reduction of the corresponding oxides were investigated by CV scanning in 0.1M NaOH solution. The potential was scanned at a

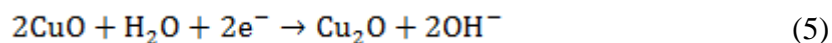
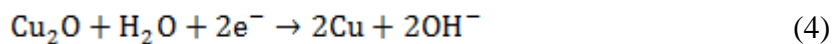
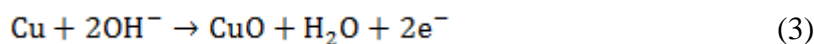
sweep rate of  $15 \text{ mV}\cdot\text{S}^{-1}$  over the potential range of  $-1.3 \text{ V (SCE)} - 0.5 \text{ V (SCE)}$ . Fig. 1 represents the first cycle of CV curve of copper in  $0.1 \text{ M NaOH}$  solution. Inspection of the curve in Fig. 1 reveals that three anodic peaks and two cathodic peaks are identified in the CV curve. There are three anodic peaks (A1, A2 and A3) prior to oxygen evolution reaction. The potential positions of anodic peaks A1, A2 and A3 are at around  $-0.41 \text{ V (SCE)}$ ,  $-0.16 \text{ V (SCE)}$  and  $0.07 \text{ V (SCE)}$  respectively. Peak A1 corresponds to the oxidation of Cu to  $\text{Cu}_2\text{O}$  monolayer formation, shown in Reaction 1. Peak A2 and Peak A3 are related to the formation of CuO in two parallel pathways, one is the oxidation of  $\text{Cu}_2\text{O}$  to CuO (Reaction 2) and another directly from Cu (Reaction 3) [20-25]. Many researchers have reported there were pores in the surface of the polarized copper in electrolytes [21, 26]. As the pores were blocked with copper oxides, the anodic current decreased, which means establishment of some passivation regions. Following that, the anodic current started to increase again as the result of conversion of  $\text{Cu}_2\text{O}$  to CuO, which is the reason of the appearance of Peak A3 [21, 26]. This process leads to an outer  $\text{CuO}/\text{Cu}(\text{OH})_2$  passive layer [20, 21, 26] and is responsible for the board passive range. Copper exhibits a typical active-passive-transpassive behavior, which is associated with the formation of duplex passive films [27]. In the reversing scan curve, Peak C1 and Peak C2 are complementary to the reduction potential positions of Peak A1 and Peak A2.



**Figure 1.** Cyclic voltammery of copper in  $0.1 \text{ M NaOH}$  solution ( $\text{pH}=9$ ) at  $25^\circ\text{C}$ .

Two cathodic peaks C1 and C2 appeared in the reverse scan curve, one is at  $-0.89 \text{ V (SCE)}$  (C1) and the other is at  $-0.57 \text{ V (SCE)}$  (C2). C1 is due to the cathodic reduction of  $\text{Cu}_2\text{O}$  to Cu (Reaction 4) and C2 comes from the cathodic reduction of CuO to  $\text{Cu}_2\text{O}$  (Reaction 5) in the electrolyte. Lenglet [28] has also assigned the first peak (C1) on the voltammogram to the reduction of  $\text{Cu}_2\text{O}$  and the second (C2) to the reduction of CuO.





Note that the characteristic reduction potentials for copper oxides are clearly separated by more than 100 mV, it indicates the coulometric reduction method can work well for compound identification of copper exposure studied here.

The other method to determine the corrosion products for the exposed copper sample is the X-ray diffraction measurements. The XRD patterns of the corrosion products are shown in Fig. 2 and the results were compared with those in the JCPDS database at the International Centre for Diffraction Data. Fig. 2(a) showed the corrosion compounds of copper after exposed 3 hours at 500°C. The peaks marked “a”, “b” and “c” match the PDF-04-0836, PDF-05-0667 and PDF-48-1548 JCPD files respectively. The files PDF-04-0836, PDF-05-0667 and PDF-48-1548 were identified to be Cu, Cu<sub>2</sub>O and CuO respectively.

After exposed at 800°C, the corrosion products of copper are easy to break into two layers. That is, the inner layer and the outer layer. The outer layer is easy to flake off from the inner layer. Fig. 2(b) represents the corrosion compounds in the inner layer of copper exposed at 800°C. The peaks marked “a” match the PDF-04-0836 JCPDS file (Cu) and the peaks marked “b” match the PDF-05-0667 JCPDS file (Cu<sub>2</sub>O). Fig. 2(c) exhibits the corrosion compounds in the outer layer of the corrosion products at 800°C. The peaks marked “b” match the PDF-05-0667 JCPDS file (Cu<sub>2</sub>O) and the peaks marked “c” match the PDF-48-1548 JCPDS file (CuO). The peaks of CuO appeared clearly in the outer layer of the corrosion product of copper. The appearance of Cu<sub>2</sub>O diffraction peak in the inner layer of the corrosion products implied the initiation of copper corrosion is the formation of Cu<sub>2</sub>O. The corrosion compounds of the layers imply there are two steps for the corrosion mechanism of copper at elevated temperature. The XRD pattern showed Cu<sub>2</sub>O but no CuO was in the inner layer of copper corrosion product, which indicated that the initiation of copper corrosion, the first step, is the formation of Cu<sub>2</sub>O, shown in Reaction 6. The second step is Cu<sub>2</sub>O converted into CuO with abundant oxygen at the outer layer, shown in Reaction 7.



The similar XRD patterns of copper as at 500°C and 800°C were observed for copper and the corrosion procedure of copper began with the growth of Cu<sub>2</sub>O whatever the temperature of exposure is. The corrosion product of copper is Cu<sub>2</sub>O accompanying with CuO at the elevated temperatures.

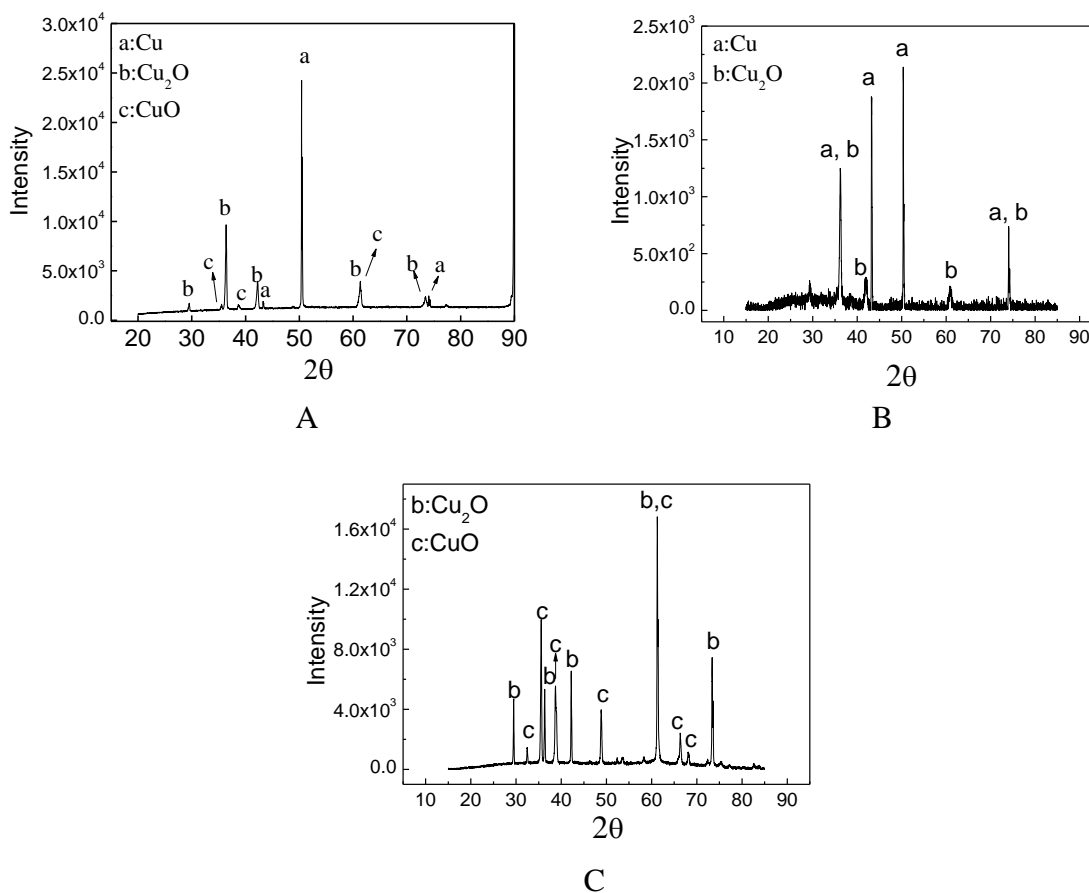
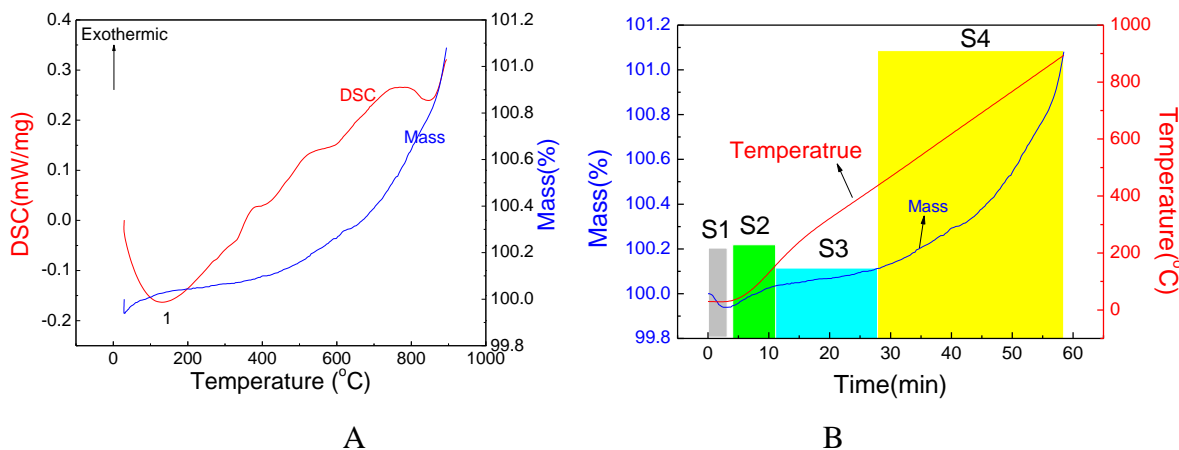


**Figure 2.** XRD diffraction patterns of the corrosion products of copper after exposed 3 hours at 500°C (a), the inner layer at 800°C (b) and the outer layer at 800°C (c).

*Isothermal-corrosion.*— A typical DSC curve of copper is shown in Fig. 3(a). TG analysis is performed with the constant heating rate of 10°C/min. In the temperature ranging from room temperature to 900°C, there is one endothermic effect and one broad exothermic effect can be easily detected: The effect 1, from room temperature to 180°C, probably corresponds to initiation corrosion of copper and the corresponding enthalpy and mass gain obviously depend on the activation energy of the samples corrosion. The effect 2, from 180-900°C, is broad and corresponds to the corrosion of copper during the thermal treatment. There are three weak effects with the maximums at around 400°C, 580°C and 845°C and probably is due to the break of the corrosion film of copper from the matrix.

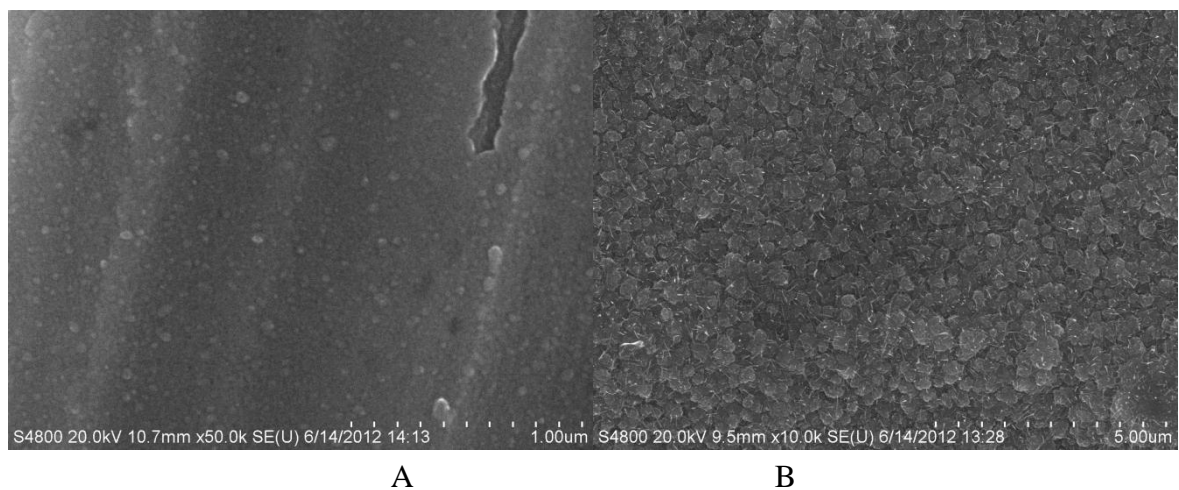
Thermograms obtained in oxidizing atmospheres for copper are shown in Fig. 3(a) and 3(b). In the atmosphere, corrosion of copper proceeds in two steps (Reaction 6 and 7) with a 1.15% mass gain over the entire temperature range (up to 900°C). During thermal treatment of the copper, mass gain occurred in four distinct stages, seen in Fig. 3(b), at consecutive temperature ranges: around room temperature (Stage 1, named S1), 30°C -80°C (Stage 2, named S2), 80°C - 180°C (Stage 3, named S3) and 180°C - 900°C (Stage 4, named S4). The stage 1 is the beginning of the thermal treatment of copper and the mass decreased with time, which corresponds to the adsorbed water and adsorbed gas on the surface of the copper sample. At the stages 2 and 3, mass of copper increased linearly with

corrosion time. While the mass of copper in the thermogravimetric analyzer increased at an exponential rate with exposure time at the stage 4. Note that the temperature is increasing with exposure time during the thermal treatment.



**Figure 3.** (a) Simultaneous TG-DSC characteristic curves of copper in a compressed air environment. (b) Mass versus time in TG measure of copper in a compressed air environment atmosphere with gas flow 20 ml/min. The temperature was controlled from room temperature to 900. The heating rate programmed at 10°C/min.

*Images of corrosion products.* – The surface morphologies of copper after exposed 3 hours at different temperatures are shown in Fig. 4. All the exposed copper samples corroded seriously whatever the temperature is. The corrosion products of the exposed copper are flaky at 100~500°C, seen in Fig. 4(a) – (c). The size of the corrosion products varies from 50 nm at 100°C (Fig. 4(a)) to micrometers at 500°C (Fig. 4(c)). The images of copper at 800°C were different from those at the lower temperatures.



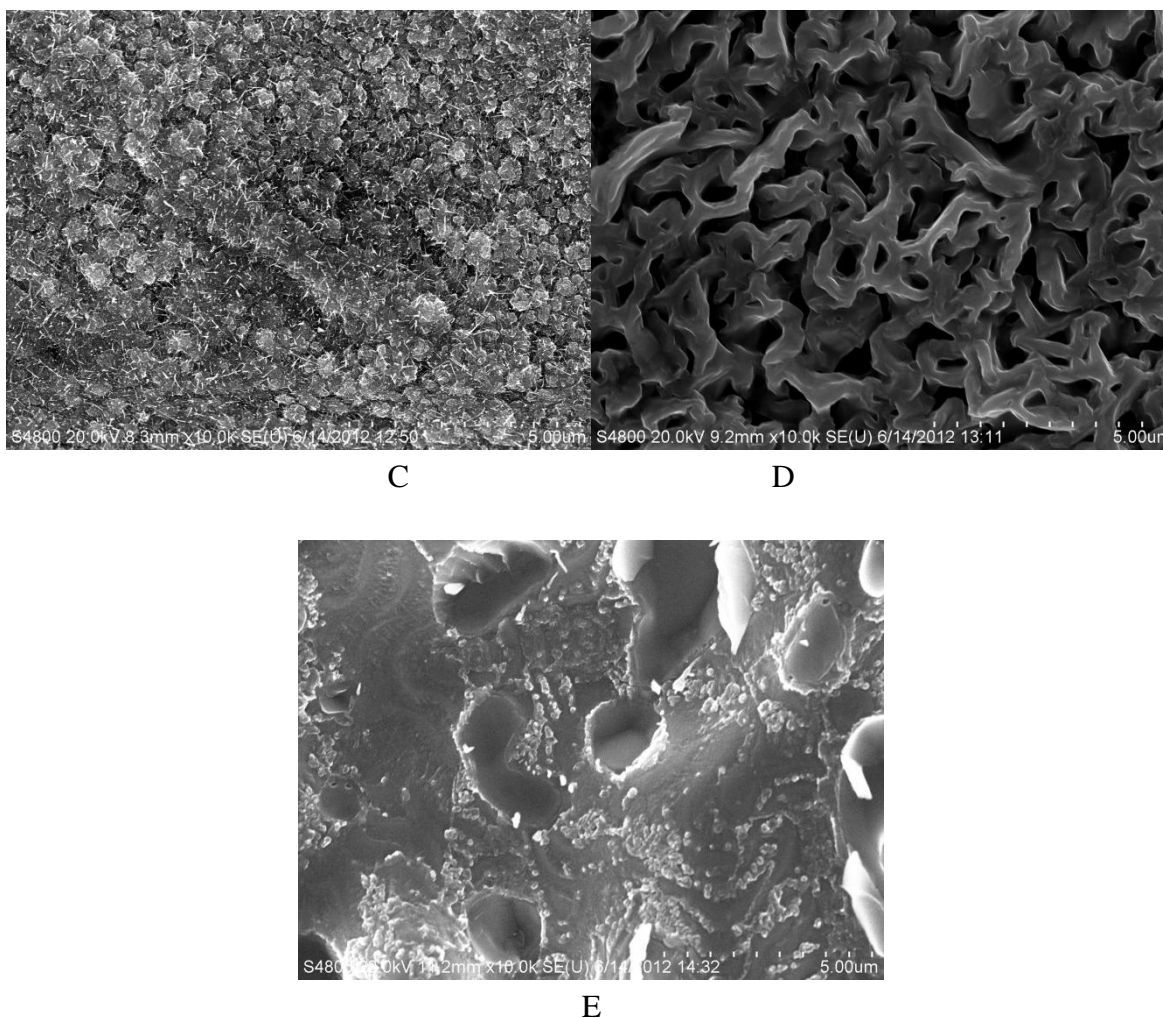


**Figure 4.** SEM images of copper after exposed 3 hours at different temperatures. (a) 100°C, (b) 300°C, (c) 500°C, (d) the outer layer of copper at 800°C and (e) the inner layer of copper at 800°C.

The morphology of outer layer of copper at 800°C showed the corrosion products were netlike porous tissues with the pore sizes of hundreds nanometers micrometer. The different corrosion images at different temperatures indicated that copper corroded with different rates at different temperatures. After about 1 hour exposure, some of the corrosion products are easy to break away from the copper sample. The two corrosion layers of the corrosion products exhibit different corrosion morphologies. After the outer layer film breaking away, intergranular corrosion can be examined and dispersed in the base copper. Many holes left on the surface of copper after the outer layer broke away, shown in Fig. 4(e). The intergranular corrosion is possibly due to thermal stress at elevated temperature.

*Corrosion kinetics.* – Coulometric reduction was performed on the exposed samples at elevated temperature in deaerated 0.1 M KCl solution at pH 9 to assess the amount of corrosion products. Coulometric reduction is an electrolytic method that measures the potential as a function of reduction time and is used to identify the compound and determine the amount present as well. As shown in Fig. 1, the reduction potentials of copper oxides are characteristic and can be used to identify copper



oxides. The corrosion behavior of copper at elevated temperature will be clear by measuring these parameters for known compounds. The parameters include the reduction potential and the reduction time, which is the duration of the potential plateaus. The duration of the reduction potentials plateau, until the reduction potential drops sharply, can be used to assess corrosion product accumulation via multiplying with the reduction current.

When copper was exposed at elevated temperature, copper oxides were formed, as demonstrated by the XRD experiment described above. The reduction curves of the exposed copper samples after exposed at the elevated temperatures are shown in Fig. 5. In order to speed up the reduction, variable reduction currents were performed because the amount of copper oxides at higher temperature was much greater than that at the lower temperatures. For example, the reduction amount of copper oxides at 800°C was much greater than that at other temperatures. Note that these variable reduction currents were only used for reductions for which the corrosion compounds were already known, as the potential shift due to the change in current density would prevent identification of the compounds. In this work, the XRD patterns have provided the corrosion compounds of copper at elevated temperatures. The reduction current was  $-0.1 \text{ mA/cm}^2$  for the copper sample exposed at 100°C and was  $-10 \text{ mA/cm}^2$  for the copper sample at 800°C because a higher current would shorten the very lengthy reduction for the copper samples with the same exposed area.

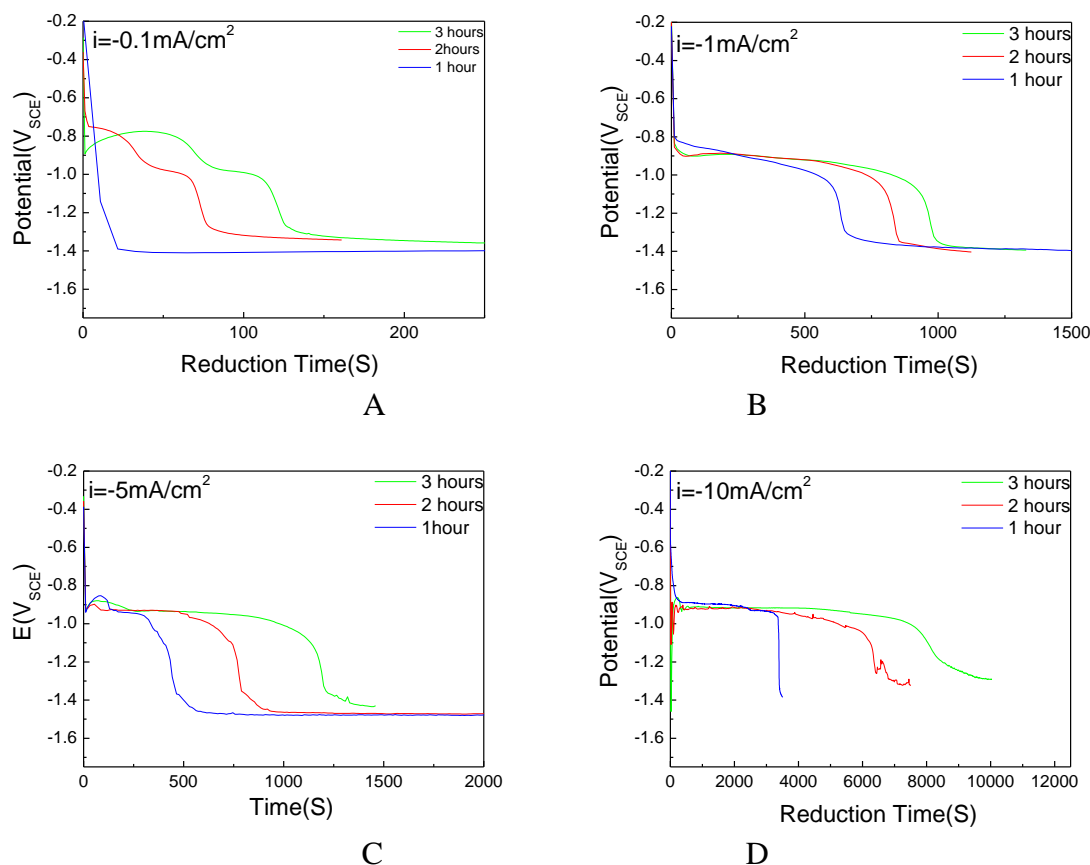


**Figure 5.** Potential versus time for coulometric reduction of the exposed copper samples in (a) 100°C, (b) 300°C, (c) 500°C, and (d) 800°C in deaerated 0.1 M KCl (pH 9) at 25°C solution.

It can be seen from Fig. 5 that during the reduction of copper after exposed at different temperature, all the samples exhibited the exact same reduction potential plateaus at approximately -0.9 V (SCE), the reduction potential for Cu<sub>2</sub>O. When the corrosion layer is completely reduced, the potential dropped sharply to approximately -1.4 V (SCE), which is the characteristic potential for water reduction on copper and indicated that the copper oxides were gone and hydrogen evolution, a new cathodic process, were occurring. When the exposure time increased, the amount of the Cu<sub>2</sub>O increased, which was observed by the larger reduction time, which is reasonable because the oxides products were flaky or porous on the surface of the copper samples. In those cases, oxygen could diffuse easily at the beginning of the exposure and encounter with fresh copper under the corrosion products later.

In order to compare the kinetics of copper corrosion at elevated temperature, the duration of the potential plateaus were chosen to calculate the reduction charges of the exposed copper by multiplying the corresponding reduction current. In this method, Q, the reduction charges of the exposed copper samples were calculated from Fig. 5 and shown in Fig. 6, which was plotted for different temperatures as a function of the exposure time. The reduction time was defined the duration from the beginning of the curves to -1.1 V (SCE), the midpoint between the adjacent reduction potentials of CuO and water.

It can be seen from Fig. 6 that the reduction charge increased with the exposure time at every exposure temperature. It can also be seen in Fig. 6 that the amount of the corrosion products was not so much and obeys linear kinetics at the elevated temperatures. The average reduction times are 10 s, 62 s and 118 s for copper after exposed 1, 2 and 3 hours respectively. Therefore, the corresponding average reduction charges (the reduction is -0.1 mA/cm<sup>2</sup>) are 1 mC, 6.2 mC and 11.8 mC respectively. The corresponding average reduction time is 454 S, 508 S and 578.5 S for the copper samples after exposed at 800°C for 1 hour, 2 hours and 3 hours respectively. The reduction current is -10 mA/cm<sup>2</sup>. Thus, the corresponding reduction charges are 33920 mC, 56000 mC and 78050 mC respectively.

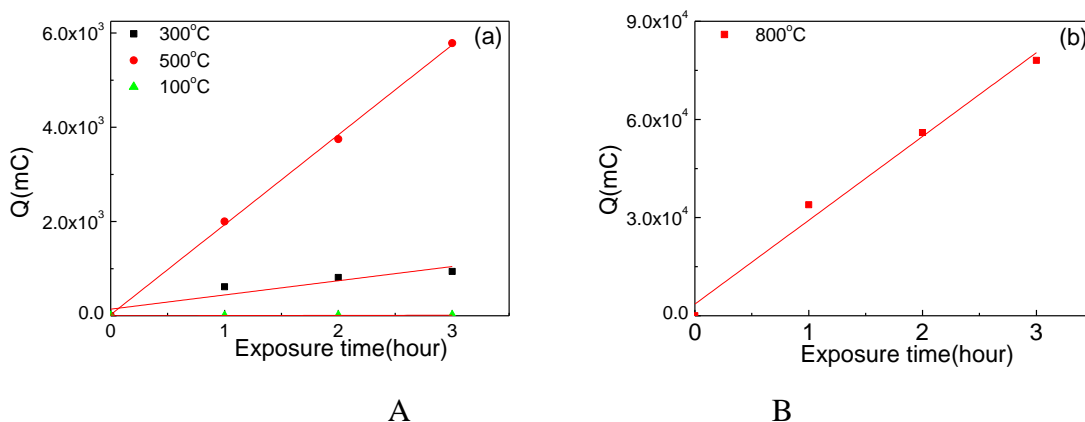
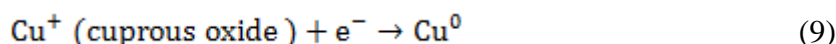


**Figure 6.** The plots are the reduction charges as the function of the exposure time at (a) 100 - 500°C and (b) 800°C. The lines are the linear fitting curves. The reduction charges were calculated from Fig.5.

#### 4. DISCUSSION

During the coulometric reduction for copper exposed at 100°C (in Fig. 5), the reduction information of CuO, seen in Reaction 8, is clear at about -0.8 V (SCE) [28]. However, at the elevated temperatures other than 100°C (in Fig. 5), no clear reduction potential at -0.8 V (SCE) was observed. Demirkan has found that some corrosion compound information was lost during the coulometric reduction as well [19]. Hollmark has observed the occurrence of Cu<sup>2+</sup> as part of a phase mixture or, alternatively, a signature for Cu<sup>(2-x)+</sup> by X-ray absorption spectroscopy [29]. The possible reason is increasing thickness of the corrosion products shifts the peak positions to more negative potentials [28] and an overlapping of Reaction 8 and Reaction 9 appeared. The results are in excellent agreement with those of Deutscher [17] and Lenglet [28].



The XRD pattern analysis in Fig. 2 has also shown that corrosion of copper leads to the formation of CuO and Cu<sub>2</sub>O on the surfaces of copper for all the exposed copper samples at elevated temperature. This result proved that there exists a significant amount of corrosion product information overlapped during the coulometric reduction process. The possible reason for the overlapping potential during the coulometric reduction is the reduction current is too big and CuO was reduced to Cu<sub>2</sub>O shortly when the samples were conducted reduction current in the electrolyte.

The plots in Fig. 6 show that elevated temperature increased the reduction charge of the exposed copper. The amount of copper corrosion increased significantly with temperature. Using one hour of exposure as an example, the corrosion amount of copper at 800°C is 33920 times of that at 100°C.

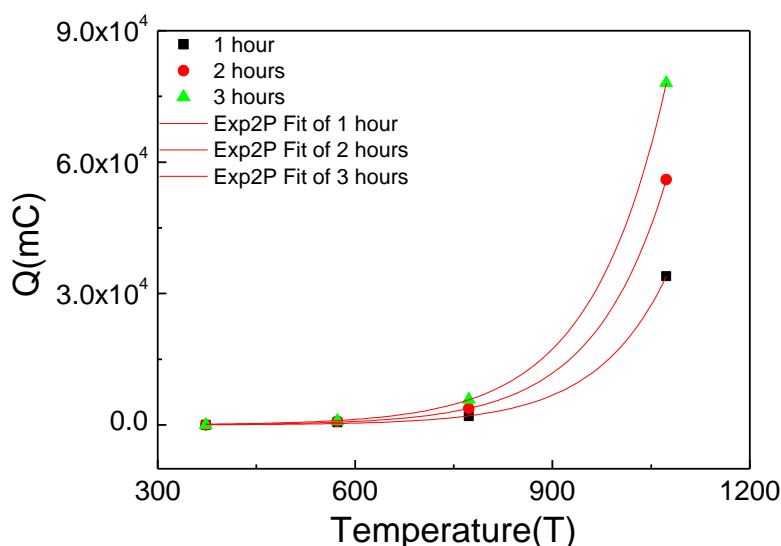


**Figure 7.** The reduction charges as the function of the exposure temperature. The reduction charges were calculated from Fig.5.

**Table 1.** Fitting parameters of Fig.6(c) with the equation  $Q = a \cdot b^T$ 

Adj. R-Square	0.99983	0.99997	0.99999
		Value	Standard Error
1 hour	a	1.58235	0.56307
1 hour	b	1.00934	3.35001E-4
2 hours	a	3.6696	0.49997
2 hours	b	1.00902	1.2825E-4
3 hours	a	6.93548	0.53651
3 hours	b	1.00873	7.28125E-5

Fig. 7 is the reduction charge of copper as the function of temperature for every exposure time to know the effect of temperature on corrosion of copper. The reduction charges were fit with exponential equation  $Q = a \cdot b^T$ . Where  $Q$  is the reduction charge and  $T$  is the exposure time.  $a$  and  $b$  are fitting parameters.  $a$  stands for the initial corrosion amount of copper and  $b$  stands for the corrosion development trend of copper with temperature. The fitting results of Fig. 6(c) are exhibited in Table 1. For the three fitting curves,  $R^2$  is bigger than 0.999, indicating the corrosion amount of copper increased exponentially with temperature at 1, 2 and 3 hours, seen in Fig. 6 (c) and Table 1.

The linear increase for the corrosion products with exposure time for every temperature in Fig. 3(b) and Fig. 6, indicates that the corrosion products are porous and allow available oxygen to diffuse up and react with the copper matrix. This conclusion is in great agreement with the images in Fig. 4.

## 5. CONCLUSIONS

Corrosion of Cu at elevated temperature has been investigated using a combination of analytical techniques, such as XRD and coulometric reduction. The corrosion rate determined by coulometric reduction and TG analysis shows a linear relationship with respect to exposure time at the beginning and an exponential kinetics with longer exposure. Temperature increases corrosion of copper exponentially. The corrosion product showed the corrosion compounds involved  $\text{Cu}_2\text{O}$  and  $\text{CuO}$  for copper at elevated temperature. Two layers of the corrosion products are formed. The inner layer of the corrosion products is mainly  $\text{Cu}_2\text{O}$  and the outer layer is made of  $\text{CuO}$  and  $\text{Cu}_2\text{O}$ . A combination of XRD and coulometric reduction allows both the amount and composition of the corrosion product to be determined.

## ACKNOWLEDGMENTS

The authors gratefully appreciate the financial support from the National Natural Science Foundation of China (Grant No.: 51101106 and 51131007) and Program for Innovative Research Team by the Ministry of Education (Grant No.: IRT1160).

## References

1. D. M. Bastidas, E. Cano, L. Bello, J. M. Bastidas, Formicary corrosion of copper tubes after two months in service. *Copper: Better Properties for Innovative Products*, 2006
2. P.J. Boden, *Corros. Sci.*, 11(1971): 363-370
3. J.H. Park, K. Natesan, *Oxid. Met.*, 39(1993): 411-435
4. M. O'Keefe, W.J. Moore, *J. Chem. Phys.*, 36 (1962): 3009-3014
5. H. L. McKinzie, M. O'Keefe, *Phys. Lett. A*, 24 (1967): 137-139
6. W.J. Tomlinson, J. Yates, *J. Phys. Chem. Solids*, 38 (1977): 1205-1206
7. E. Iguchi, K. Yajima, Y. Saito, *Trans. Jpn. Inst. Met.*, 14 (1973): 423-430
8. J. Sestak, *Thermophysical Properties of Solids*, Elsevier, Amsterdam, 1984
9. J. Li, F.X. Zhang, Y.W. Ren, Y.Q. Hun, Y.F. Nan, *Thermochim. Acta*, 406 (2003): 77-87
10. S. Mrowec, A. Stoklosa, *Oxid. Met.*, 3 (1971): 291-311
11. J.H. Park, K. Natesan, *Oxid. Met.*, 39 (1993): 411-435
12. M. O'Reilly, X. Jiang, J.T. Beechinor, S. Lynch, C. NiDheasuna, J.C. Patterson, G.M. Crean, *Appl. Surf. Sci.*, 91(1995): 152-156
13. H. Tanaka, N. Koga, A.K. Galwey, *J. Chem. Educ.*, 72 (1995): 251- 256
14. N. Koga, H. Tanaka, *Thermochim. Acta*, 303 (1997): 69-76
15. 'Standard test method for coulometric reduction of surface films on metallic test samples', in 'Annual book of ASTM standards', ASTM B825, ASTM, Philadelphia, PA, 2007
16. R.H. Lambert, D. J. Trevo, *J. Electrochem. Soc.*, 105 (1958) 18
17. R.L. Deutscher, R. Woods, *J. Appl. Electrochem.*, 16 (1986) 413
18. Sungkyu Lee, Roger W. Staehle, Coulometric reduction of oxides formed on copper, nickel and iron, *J. Electrochem. Soc.*, 142 (1995): 2189-2195
19. K. Demirkan, G. E. Derkits, Jr., D. A. Fleming, J. P. Franey, K. Hannigan, R. L. Opila, J. Punch, W. D. Reents, Jr., M. Reid, B. Wright, C. Xu, *J. Electrochem. Soc.*, 157 (2010): C30-C35
20. S.S.A. EIRehim, E.E. Foad, *Collect. Czech. Chem.C.*, 61 (1996): 85-92
21. F.H. Assaf, A.M. Zaky, S. S. Adb EI-Rehim, *Appl. Surf. Sci.*, 187 (2002): 18-27
22. R. Subramanian, V. Lakshminarayanan, *Corros. Sci.*, 44, (2002): 535-554
23. S.M.A. Elhaleem, B. G. Ateya, *J. Electroanal. Chem.*, 117 (1981): 309-319
24. S. Fletcher, R.G. Barradas, J.D. Porter, *J. Electrochem. Soc.*, 25 (1978): 1960-8
25. J.M.M. Droog, C.A. Alderliesten, P.T. Alderliesten, G.A. Bootsma, *J. Electroanal. Chem. Interfacial Electrochem.*, 111(1980): 61-70
26. D.W. Shoesmith, S. Sunder, M.G. Bailey, G.J. Wallace, F.W. Stanchell, *J. Electroanal. Chem. Interfacial Electrochem.*, 143 (1983): 153-165
27. F. Rosalbino, R. Carlini, F. Soggia, G. Zanicchi, G. Scavino, *Corros. Sci.*, 58 (2012): 139-144
28. M. Lenglet, K. Kartouni, D. Delahaye, *J. Appl. Electrochem.*, 21 (1991): 697-702
29. H.M. Hollmark, P.G. Keech, J.R. Vegelius, L. Wermea, L.-C. Duda, *Corros. Sci.*, 54 (2012): 85-89